Propagation effects in apertureless near-field optical antennas

Kanglin Wang, Adrian Barkan, and Daniel M. Mittleman[a)]
Rice University, Department of Electrical and Computer Engineering, MS 366, Houston, Texas 77251-1892

(Received 8 September 2003; accepted 17 November 2003)

We report a direct observation of the electromagnetic wave propagation on optical antennas. A free-space broadband terahertz pulse is coupled into a propagating mode along the shaft of an optical antenna acting as an apertureless near-field probe. We determine the spatial extent of this guided mode and its velocity. In addition, we consider the possibility of multiply reflected modes propagating along the near-field probe, an effect which will be significant in near-field spectroscopic measurements. © *2004 American Institute of Physics.* [DOI: 10.1063/1.1640473]

Since the study of infrared whisker diodes in the 1970s,[1] the use of antennas as optical devices has drawn increasing attention from various research fields. In recent years, optical antennas have been discussed as a promising tool for use in near-field optical microscopy (NSOM) due to their ability to concentrate electromagnetic waves in a subwavelength region.[2,3] A metallic probe tip is one of the most widely used forms of this kind of antenna.[4,5] To describe the near-field response of the antenna, the probe tip is often modeled as a tiny scattering sphere with a size determined by the tip's radius of curvature.[4,6] However, it has been found that not only the probe apex but also the probe shaft and the shape of the whole tip structure play important roles in experiments.[7,8] One reason for this is easy to understand: it is very difficult to focus the incident beam only on the probe apex and not on the shaft, especially for infrared and microwave sources. A concern which immediately arises is the influence of propagation effects of the incident radiation along the probe tip. These effects can influence the phase of the electric field scattered from the tip, and therefore have an impact on interferometric apertureless microscopy[4,7,9] and also on the growing field of near-field optical spectroscopy.[8,10,11] Thus, it is important to characterize the effects of propagation on the measured signals in apertureless NSOM.

Here, we report a direct observation of the electromagnetic wave propagation on apertureless near-field optical antennas, measured in the time domain. The method we use is a combination of a typical apertureless NSOM configuration[5,6] with terahertz (THz) time-domain spectroscopy.[12–14] This technique is advantageous here because it permits coherent detection of the electric field of THz pulses, and therefore provides a direct measurement of phase distortions induced by the probe tip. We also note that apertureless NSOM techniques have only very recently been explored at terahertz frequencies.[15,16]

The broadband single-cycle pulses of free-space THz radiation used in our measurements are generated and coherently detected using ultrafast photoconductive gating.[12–14] The schematic of our experimental setup is shown in Fig. 1. THz pulses are focused onto a beryllium–copper needle acting as a near-field probe, with a shaft of 0.5 mm diameter and a tip of about 25 μm radius. The sample is a featureless gold-coated silicon wafer, placed in close vicinity of the tip. The mean distance between the tip and the gold surface, $d \sim 350$ nm, is precisely controlled by a piezoelectric transducer. In such a configuration, the tip strongly interacts with its image in the metal surface, and converts the localized evanescent field around the tip to propagating radiation through a scattering process.[6] The scattered radiation is modulated at 750 Hz by vibrating the probe tip normal to the surface, and demodulated using a lock-in amplifier.[5,9]

In experiments of this sort, it is not possible to focus the THz beam onto the surface without also illuminating the metal probe shaft. As a result, some of the radiation is coupled into a propagating mode on the shaft of the probe, which acts as an antenna. The propagating mode excites the tip, and produces a scattered wave which is detected by the THz receiver. As shown in Fig. 1, the THz transmitter and the focusing lenses are mounted on a movable stage so that the incident position along the shaft can be controlled.

In Fig. 2(a) we plot a series of time-domain THz pulses, obtained by moving the transmitter stage along the shaft of the needle in steps of 1.5 mm. The propagation effect is evident from the relative delay of these wave forms. As the point of incidence moves away from the tip, the pulse takes longer to propagate along the shaft, and its amplitude decreases. From Fig. 2(b), it is clear that this propagation is largely nondispersive, since the shape of the time-domain

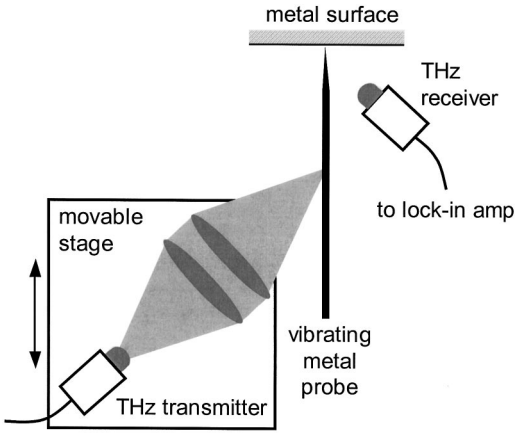

FIG. 1. A schematic of the experimental setup. THz pulses are focused onto a vibrating probe. The focal spot can be moved along the shaft of the probe. The propagating pulse is detected using a photoconductive receiver.

[a)]Electronic mail: daniel@rice.edu

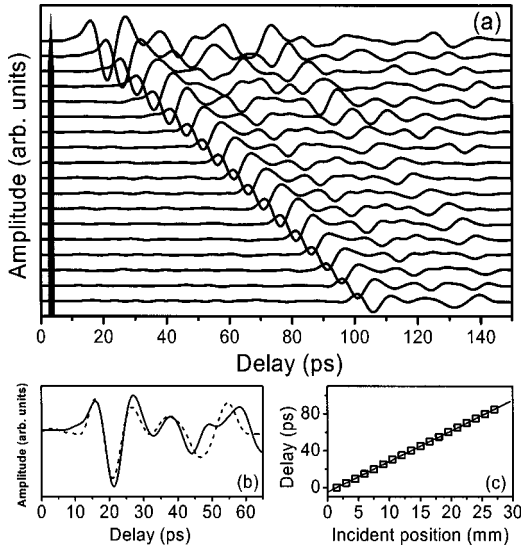

FIG. 2. (a) A series of time-domain THz pulses, for different positions of the incident beam focus on the probe shaft. Each successive wave form corresponds to a translation of the beam spot by 1.5 mm. (b) A close-up view of the upper and lower wave forms shown in (a). Here, the lower wave form has been shifted to smaller delays and scaled by a constant factor (dashed curve), to facilitate comparisons with the upper wave form (solid curve). Other than attenuation, there is little pulse reshaping, which indicates that the propagating mode is largely dispersionless. (c) Arrival time vs incidence position, with a least-squares linear fit to the data. The slope of this line is the group velocity of the guided mode, essentially equal to the vacuum speed of light.

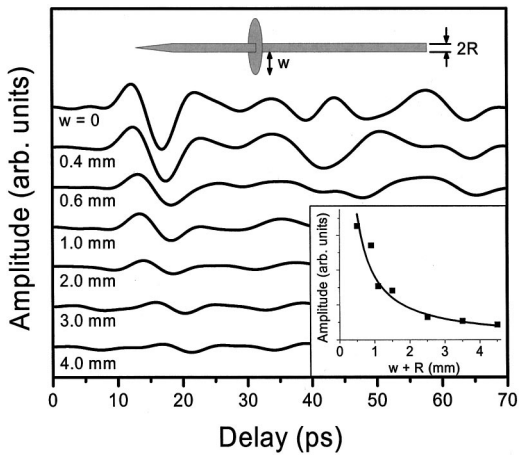

FIG. 3. THz pulses measured with a circular aluminum barrier situated between the incident position and the probe tip, for several different barrier sizes. The inset shows the peak-to-peak amplitude vs barrier size, along with a least-squares fit to $1/r$.

wave form does not depend strongly on propagation distance. We note that the shape of the detected THz pulse is different from that of the incident THz pulse due to the near-field response of the probe tip. These details will be described in a separate publication.

In order to characterize the phase distortions introduced by the propagation along the probe shaft, we first determine the group velocity of the propagating mode. As shown in Fig. 2(c), the propagation delay is a linear function of the propagation distance. A least-squares fit to these data yields the group velocity of the propagating mode, $v_G = 0.300 \pm 0.001$ mm/ps, equivalent to the free-space velocity c. This result, together with absence of pulse broadening and low-frequency cutoff, suggests that the propagating mode is a low-order transverse electric and magnetic (TEM) mode, similar to the lowest order mode of a coaxial waveguide. We note that the attenuation of the TEM mode in a coaxial waveguide is predicted to vanish in the limit that the inner radius of the outer conductor diverges, even if the conductors are not ideal metals.[17] However, in our data, we observe some attenuation, $\mathrm{Im}(\beta) \sim 0.25\ \mathrm{cm}^{-1}$. This discrepancy may be a result of the fact that the conventional analysis of coaxial modes assumes that the wavelength of the radiation is much larger than the dimensions of the waveguide. This is only approximately true in our experiment, so a more rigorous analysis is probably required to accurately determine the modal pattern and the conductivity losses. We note that the probe shaft used in our experiment is coated with a thin layer of tin to prevent oxidation. This layer, which is thicker than the skin depth for the relevant frequency range, has a resistivity that is more than six times that of copper.

To study the spatial distribution of this propagating mode, we perform a more detailed measurement by adding aluminum barriers of different radii onto the probe, in order to impede the propagation of the mode (see Fig. 3). The barrier is located 11.7 mm away from the tip, and the THz beam is focused on a spot 27 mm away from the tip. As the size of the barrier increases, the amplitude of the detected THz pulse decreases, as roughly $1/r$. We conclude that the propagation mode is mainly localized within ~ 1 mm around the shaft. We also observe a slight decrease in the bandwidth of the detected THz pulses with the increasing barrier size, showing that higher frequency components have smaller spatial extent in this mode.

In order to emphasize the significance of these results in the context of broadband apertureless NSOM, we consider the possibility of multiple reflections of the waveguide mode. It is easy to imagine that any discontinuity in the waveguide, such as the sort shown in Fig. 3, could generate a reflected wave, leading to the possibility of multiple time-delayed scattered pulses reaching the detector. In this case, the spectrum of the received radiation would be modulated by the presence of these multiple reflections, in analogy to the Fabry–Pérot effect. This modulation could complicate the interpretation of spectroscopic measurements. Figure 4 illustrates this effect. The incident pulse is focused on the probe tip, and the receiver detects the scattered radiation. At the same time, the incident radiation is also coupled to a propagating mode and move away from the sample along the probe shaft. Upon reaching the metal barrier, this propagating wave is partially reflected and moves back towards the tip. This process can repeat until the propagating wave dissipates. Additional scattered pulses are generated each time the propagating wave reaches the probe tip. In the comparison of the detected THz pulse with barrier to that without barrier, the reflected transients are evident, indicated with arrows in Fig. 4. The relative delays of these peaks precisely coincide with the round-trip propagation time between the barrier and the probe tip at velocity c.

In summary, we have observed the effects of guided propagation on a near-field optical antenna. By detecting the propagating THz pulses in the time domain with an apertureless NSOM configuration, the propagation is characterized as

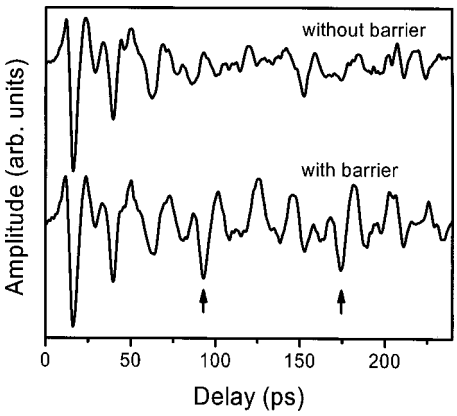

FIG. 4. THz pulses detected with direct illumination of the probe tip. The upper wave form is obtained with no barrier on the probe, while the lower wave form is obtained with an aluminum barrier ($w=3$ mm) on the probe, as in Fig. 3. The barrier gives rise to multiply reflected guided modes, which are indicated by arrows.

a localized mode in the vicinity of the probe shaft. Understanding these propagation effects will be important for near-field microscopy studies which involve the phase of the scattered optical radiation. In addition, the effect of multiple reflections can substantially perturb the spectrum of the measured signal, which would be significant for near-field spectroscopy. This is likely to be important in experiments where structures in the optical setup can act as a reflector, such as a probe holder or an atomic force microscopy cantilever.

This work was supported in part by Advanced Micro Devices and by the R. A. Welch Foundation.

[1] L. M. Matarrese and K. M. Evenson, Appl. Phys. Lett. **17**, 8 (1970).
[2] R. D. Grober, R. J. Schoelkopf, and D. E. Prober, Appl. Phys. Lett. **70**, 1354 (1997).
[3] K. B. Crozier, A. Sundaramurthy, G. s. Kino, C. F. Quate, D. P. Fromm, and W. E. Moerner, *Quantum Electronics & Laser Science Conference* (Optical Society of America, Washington DC, 2003), paper QTuD3.
[4] F. Zenhausern, Y. Martin, and H. K. Wickramasinghe, Science **269**, 1083 (1995).
[5] Y. Inouye and S. Kawata, Opt. Lett. **19**, 159 (1994).
[6] B. Knoll and F. Keilmann, Nature (London) **399**, 134 (1999).
[7] R. Hillenbrand and F. Keilmann, Phys. Rev. Lett. **85**, 3029 (2000).
[8] L. Aigouy, F. X. Andréani, A. C. Boccara, J. C. Rivoal, J. A. Porto, R. Carminati, J.-J. Greffet, and R. Mégry, Appl. Phys. Lett. **76**, 397 (2000).
[9] F. Zenhausern, M. P. O'Boyle, and H. K. Wickramasinghe, Appl. Phys. Lett. **65**, 1623 (1994).
[10] J. Seidel, S. Grafström, Ch. Loppacher, S. Trogisch, F. Schlaphof, and L. M. Eng, Appl. Phys. Lett. **79**, 2291 (2001).
[11] R. Hillenbrand, T. Taubner, and F. Keilmann, Nature (London) **418**, 159 (2002).
[12] M. van Exter and D. Grischkowsky, IEEE Trans. Microwave Theory Tech. **38**, 1684 (1990).
[13] P. R. Smith, D. H. Auston, and M. C. Nuss, IEEE J. Quantum Electron. **24**, 255 (1988).
[14] D. M. Mittleman, R. H. Jacobsen, and M. C. Nuss, IEEE J. Sel. Top. Quantum Electron. **2**, 679 (1996).
[15] N. C. J. van der Valk and P. C. M. Planken, Appl. Phys. Lett. **81**, 1558 (2002).
[16] H.-T. Chen, R. Kersting, and G. C. Cho, Appl. Phys. Lett. **83**, 3009 (2003).
[17] N. Marcuvitz, *Waveguide Handbook* (Peter Peregrinus, London, 1986).